OsteoArthritis and Cartilage (2006) **14,** 477–485

doi:10.1016/j.joca.2005.11.011

Osteoarthritis and Cartilage

International Cartilage Repair Society

OARSI OSTEOARTHRITIS RESEARCH SOCIETY INTERNATIONAL

Premature osteoarthritis in the Disproportionate micromelia (*Dmm*) mouse[1]

B. D. Bomsta M.S.†, L. C. Bridgewater Ph.D.‡ and R. E. Seegmiller Ph.D.†*

† *Department of Physiology and Developmental Biology, Brigham Young University, Provo, UT 84602, USA*

‡ *Department of Microbiology and Molecular Biology, Brigham Young University, Provo, UT 84602, USA*

Summary

Objective: Degeneration of articular cartilage leads to the development of osteoarthritis (OA), but the molecular pathology of the disease is poorly understood. The Disproportionate micromelia (*Dmm*) mouse has a deletion mutation in the C-propeptide encoding region of *Col2a1*, which leads to a defective cartilage matrix. The objective of this study was to determine whether heterozygous (*Dmm*/+) mice develop premature OA, and could therefore serve as an animal model for studying the molecular pathways leading to OA.

Design: Histological analysis was utilized to determine the state of articular cartilage degeneration in *Dmm*/+ mice at 3, 6, 9, 12, 15, and 22 months of age. Severity of OA was quantified with a modified Mankin scoring system. In addition, articular cartilage thickness, cell density, and the extracellular matrix (ECM) fraction of articular cartilage were quantified.

Results: Articular cartilage erosion was significantly more severe in *Dmm*/+ than in wild-type (+/+) mice beginning at 9 months, and modified Mankin scoring revealed *Dmm*/+ articular cartilage to be in a more severe osteoarthritic state as early as 3 months. In addition, *Dmm*/+ articular cartilage was thinner than +/+ cartilage and showed increased cell density and decreased matrix fraction compared with +/+ from the earliest time points measured.

Conclusions: The present study demonstrates that *Dmm*/+ mice develop premature OA. The observed degenerative changes of *Dmm*/+ articular cartilage closely resemble those of human OA patients, with or without *Col2a1* mutations, suggesting that *Dmm*/+ mice are a useful model for investigating mechanisms involved in OA.

Key words: Disproportionate micromelia *Dmm*, Osteoarthritis, Articular cartilage, Cartilage erosion, *Col2a1*, Type II collagen.

Introduction

Osteoarthritis (OA), characterized by painful degeneration of articular cartilage and dysfunction of joints, affects 21 million people in the United States alone and is a leading cause of disability in this country[1]. Risk factors for the development of OA include age, obesity, joint injuries, excessive joint use, and hereditary conditions including malformed joints and defective cartilage[1]. However, in spite of the large number of people affected and the broad distribution of risk factors in the population, the molecular pathogenesis of the disease is not yet well understood. Therefore, there is a critical need for the development and study of appropriate and convenient animal models of OA, both for expanding our understanding of the disease and for developing and testing new treatments.

Much of the animal research on OA performed to date has utilized large animals such as dogs, rabbits, sheep, and pigs in which OA results from surgical instability induced by partial or total meniscectomy, by anterior cruciate transaction, or by surgically applied damage[2–4]. OA has also been induced in large animals by intra-articular injection of iodoacetate or collagenase[5,6]. These large animal models have yielded useful information about the progression of OA and have been utilized to test potential treatments, but the difficulty of maintaining large research animals makes such experiments impractical for the vast majority of laboratories. Rodent models of OA are much more useful and practical for most researchers.

A few mouse models of OA are currently available. One of these, STR/ort, has been studied since the late 1970s[7–9]. STR/ort mice spontaneously develop premature OA, with manifestations including articular cartilage erosion, thickening of the subchondral bone, and widespread calcification within the knee joints. Unfortunately, the genetic basis for this predisposition to OA is not known. A second model, Del1, was created by transgenically introducing a mutated *Col2a1* gene into the C57BL background[10]. The mutated gene contains a 45 bp deletion within the triple helical coding region, and its overexpression causes subchondral bone sclerosis, cartilage erosion, fragmented menisci, and osteophyte formation[11]. A third model, the chondrodysplasia (*cho*) mouse, contains a single nucleotide deletion mutation in the *Col11a1* gene, which leads to a premature stop codon[12]. This naturally occurring mutation causes premature onset OA as evidenced by chondrocyte clustering, proteoglycan loss, and degradation of type II collagen at the articular surface[13,14].

We demonstrate herein that the murine line called Disproportionate micromelia (*Dmm*) can also serve as a useful new animal model of OA. Research begun in the early

[1]This research was supported by National Institute of Health grants AR 47568 (to R.E.S) and AR 48839 (to L.C.B).

*Address correspondence and reprint requests to: Robert E. Seegmiller, Ph.D., Department of Physiology and Developmental Biology, 593 WIDB, Brigham Young University, Provo, UT 84602, USA. Tel: 1-801-422-2303; Fax: 1-801-422-0700; E-mail: robert_seegmiller@byu.edu

Received 20 October 2005; revision accepted 21 November 2005.

1980s has demonstrated that homozygous (*Dmm*/*Dmm*) mice display severe skeletal dysplasia and cleft palate secondary to micrognathic tongue obstruction, and die shortly after birth due to pulmonary hypoplasia caused by rib skeletal dysplasia[15–17]. Heterozygotes (*Dmm*/+), in contrast, appear normal at birth and exhibit only mild dwarfism beginning at approximately 1 week postpartum[15].

The *Dmm* mutation is a three-nucleotide deletion in the C-propeptide coding region of the *Col2a1* gene, which replaces lysine and threonine with asparagine (KT206,207N) in a highly conserved region of the protein[18]. Although the C-propeptide region is not part of the mature type II collagen molecule, it plays an important role in collagen trimer assembly. After proα1(II) chains, coded by the *Col2a1* gene, are translated and secreted into the rough endoplasmic reticulum (RER), the C-propeptides associate via hydrophobic and electrostatic interactions, with assistance from specific protein chaperones[19,20]. Subsequently, intra- and interchain disulfide bonds form that help stabilize the homotrimer during folding of the triple helical domains[21,22]. Once folding is accomplished, proα1(II) trimers are transported to the extracellular matrix (ECM) where their N- and C-propeptides are enzymatically cleaved and the triple helical domains are incorporated and cross-linked into the heterotypic fibers[21]. In the *Dmm* mouse, the C-propeptide mutation prevents normal collagen processing, resulting in the accumulation of type II collagen intracellularly, with a corresponding deficiency of this protein in the cartilage ECM[23].

Similar mutations in the human *COL2A1* gene have been shown to cause a variety of disease phenotypes in cartilage[24]. Although the majority of identified *COL2A1* mutations disrupt the repetitive Gly-X-Y pattern of amino acids in the triple helical domain, five disease-causing mutations have been identified in the C-propeptide coding region of *COL2A1*. They all cause phenotypically overlapping chondrodysplasias: Stickler syndrome[25], vitreoretinopathy with phalangeal epiphyseal dysplasia[26], spondyloperipheral dysplasia, achondrogenesis II − hypochondrogenesis, and spondyloepiphyseal dysplasia[25–29]. Furthermore, all are associated with degeneration of the articular cartilage. As in *Dmm* mice, the C-propeptide mutations are presumed to cause disease phenotypes by producing chains that disrupt the assembly and/or secretion of triple helical procollagen molecules[18,23].

The phenotypic similarities between the human *COL2A1* C-propeptide mutations and the *Dmm* mutation suggested that the *Dmm* mouse would be a useful model for the study of OA. We present here a thorough histological analysis of articular cartilage abnormalities in *Dmm*/+ mice and demonstrate that these mice do, in fact, display most of the histological hallmarks of OA including articular cartilage thinning and degeneration, proteoglycan loss, increased cell density, and decreased ECM. The *Dmm*/+ mouse, therefore, has potential as a new model of OA for the study of disease progression and for the development and testing of OA treatments.

Methods

FACILITIES, EXPERIMENTAL ANIMALS, AND GENOTYPING

The animals used in this study were maintained in the animal care facility of Brigham Young University. Mice were kept in paper-bedded, 5.7 L cages, fed a typical mouse diet, and provided with a 12-h-light/12-h-dark cycle.

Heterozygous mice (*Dmm*/+) on a C3H strain background were crossed to produce the wild-type (+/+) and *Dmm*/+ mice used in this study. Approximately 1 month postpartum, the pups were isolated from the dam and assigned a number, and marks representing each number were punched into each animal's ears for identification throughout the study. Tail samples were obtained at this time for use in genotyping.

DNA was isolated from the tail samples, and polymerase chain reaction (PCR) amplification was performed with primers flanking the mutation site, followed by restriction enzyme digestion with *Bcg*I, a restriction enzyme that recognizes the mutated nucleotide sequence but not the wild-type sequence[18]. Restriction fragments were separated on a 1% agarose gel containing ethidium bromide and viewed with a UV transilluminator.

TISSUE PROCESSING

Mice of each genotype at various ages (3, 6, 9, 12, 15, and 22 months) were weighed, asphyxiated with CO_2, and the left knee joint was removed from each mouse. These joints were fixed in periodate−lysine−paraformaldehyde, decalcified in formic acid, and embedded in paraffin. Paraffin blocks containing the joints were then prepared with each knee bent at a 120° angle, the tibia parallel to the sectioning surface, and the femur obliquely perpendicular to the sectioning surface. These tissue blocks were cut into 6-μm-thick serial sections through the entire joint, starting at the anterior surface, thereby yielding six 210-μm-thick strata [Fig. 1(A)]. With the tissue thus oriented in the blocks, we were able to examine each quadrant of the knee joint in the coronal section [Fig. 1(B)], including medial and lateral tibial plateaus and medial and lateral femoral condyles. One slide from each stratum was stained with hematoxylin and eosin and another was stained with safranin O and fast green. Hematoxylin and eosin-stained tissue was analyzed to determine articular cartilage thickness [Fig. 1(C)] and the extent of cartilage erosion (Table I). The fast green and safranin O-stained tissue was used to assess the osteoarthritic state of the cartilage using a modified Mankin scoring system (Table I).

Additional left knee joints from 3- and 6-month mice were fixed in 3% glutaraldehyde in 0.1 M phosphate buffer, decalcified in L-ascorbic acid, bisected sagittally through the patellar notch, postfixed in 1% osmium tetroxide, and embedded in Spurr's Low Viscosity Embedding Resin. The medial portion of each joint was oriented with the cut surface parallel to the sectioning surface of the block, oriented such as to yield sagittal sections. Each plastic block was cut into 1-μm-thick sagittal sections and stained with toluidine blue/azure II solution. These tissue sections were used to determine cell density and to estimate the matrix fraction of articular cartilage. All slides containing stained sections were viewed and photographed under an Olympus BX51 light microscope attached to a computer-operated Spot RT digital color camera.

QUANTIFICATION OF EROSION AND THICKNESS OF ARTICULAR CARTILAGE

Hematoxylin and eosin-stained tissue was examined under the microscope and an erosion score was determined for each quadrant of each stratum of each joint, depending on how deep the erosion extended into the cartilage[1,11,30]. Scores were assigned as shown in Table I. With this scoring system, a higher erosion score corresponded to more severe OA. The average erosion score for each joint was then calculated.

Sections from each stratum of each knee joint were photographed and the digital images were analyzed using Adobe

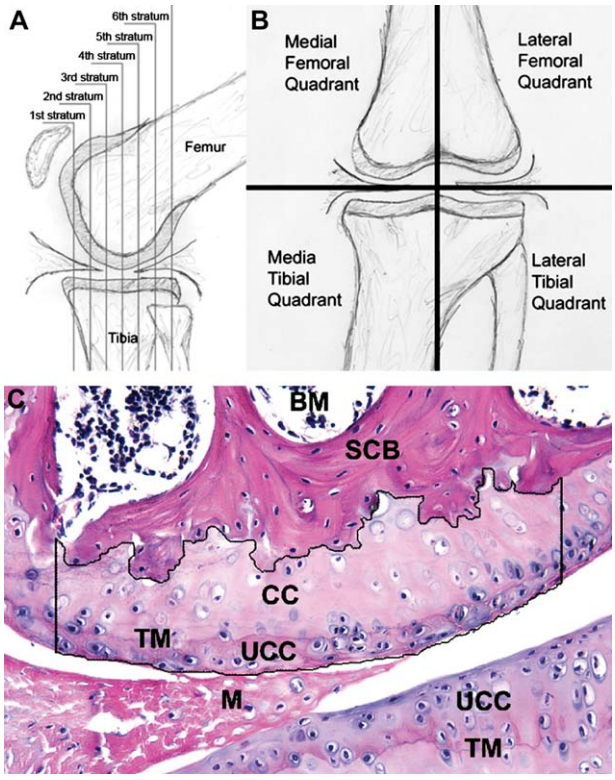

Fig. 1. (A and B) Schematic representation of left knee joints showing the divisions used in this study. (A) Lateral view. Vertical lines represent the borders between each of the strata. (B) Anterior view. Black lines indicate borders between each of the quadrants. (C) Illustration of the method by which cartilage thickness was quantified. Adobe Photoshop's selection tools were used to select an area that spanned 500 μm across the surface of the cartilage and extended down to the surface of the subchondral bone. The selected area is shown within the thin black line. The number of pixels within the area was converted to μm^2 and this value was divided by 500 μm to estimate the average cartilage thickness within the selected area. BM, bone marrow; SCB, subchondral bone; CC, calcified cartilage; TM, time mark; UCC, uncalcified cartilage; M, meniscus.

Photoshop 7.0 (Adobe Systems, San Jose, CA). Photoshop's selection tools were used to select an area that spanned 500 μm across the surface of the cartilage and extended down to the surface of the subchondral bone [Fig. 1(C)]. The number of pixels in the selected area was noted in Photoshop's histogram window. This value was then converted to μm^2 and divided by 500 μm to provide an estimate of the average overall thickness of the cartilage (measured from cartilage surface to the subchondral bone) within the selected area. This procedure was also used to determine the average thickness of uncalcified cartilage, in which the area selected extended down to the tidemark. We then mathematically determined the thickness of calcified cartilage. This procedure was done for each quadrant of each stratum of each joint.

DETERMINATION OF OA SEVERITY

Safranin O and fast green-stained tissue was examined under the microscope and scores were assigned based on three criteria: interterritorial matrix staining (IMS) of uncalcified cartilage with safranin O, pericellular matrix staining (PMS) with safranin O, and spatial arrangement of chondrocytes (SAC). Scores for each of these three criteria were assigned as shown in Table I. The assigned subscores from each of these criteria were summed to determine the modified Mankin score for each quadrant of each stratum of each knee joint [1,14,30]. With this technique, a higher score indicates a more severe state of OA. The average score for each joint was then calculated.

Table I
Scoring systems used to evaluate articular cartilage of mice

Feature	Score
Cartilage erosion scoring system	
Smooth noneroded cartilage	0
Rough noneroded cartilage	1
Superficial fibrillation	2
Separation of uncalcified from calcified cartilage	3
Erosion of uncalcified cartilage only	4
Erosion extending into calcified cartilage	5
Erosion down to the subchondral bone	6
Modified Mankin scoring system	
PMS	
Normal intensity	0
Focal points of enhanced intensity	1
More than 40% of cartilage with enhanced staining	2
SAC	
Normal	0
Diffuse hypercellularity	1
Focal points of hypocellularity	2
Diffuse hypocellularity	3
IMS	
Normal staining	0
Reduced staining	1
Focal points without any staining	2
More than 40% of cartilage without any staining	3

DETERMINATION OF CELL DENSITY AND MATRIX FRACTION

Toluidine blue/azure II stained tissue was photographed, and the digital images were analyzed using Adobe Photoshop 7.0 (Adobe Systems, San Jose, CA). An area that spanned 1 mm across the surface of the medial femoral cartilage and extending through the depth of the cartilage bordering the subchondral bone was selected, and the size of this area was determined. The cells within the area were then counted to estimate cell density, and the area occupied by these cells was subtracted from the total area to determine the matrix fraction of the selected tissue field.

STATISTICAL ANALYSIS

A two-way analysis of variance (ANOVA) was used to compare the means of *Dmm*/+ data from the entire joint (erosion scores, total cartilage thickness, cell density, matrix fraction, and modified Mankin scores) in relation to age, with the means of +/+ data. Student's *t* test was used to compare the means of calcified cartilage thickness, uncalcified cartilage thickness, IMS sub-scores, PMS subscores, and SAC sub-scores from *Dmm*/+ cartilage with those of age-matched +/+ cartilage.

Results

EROSION OF *DMM*/+ CARTILAGE

Inspection of +/+ knee joints showed healthy articular cartilage with little or no erosion through 22 months (Fig. 2). *Dmm*/+ knee joints revealed erosion of uncalcified cartilage by 6 months of age and erosion to the

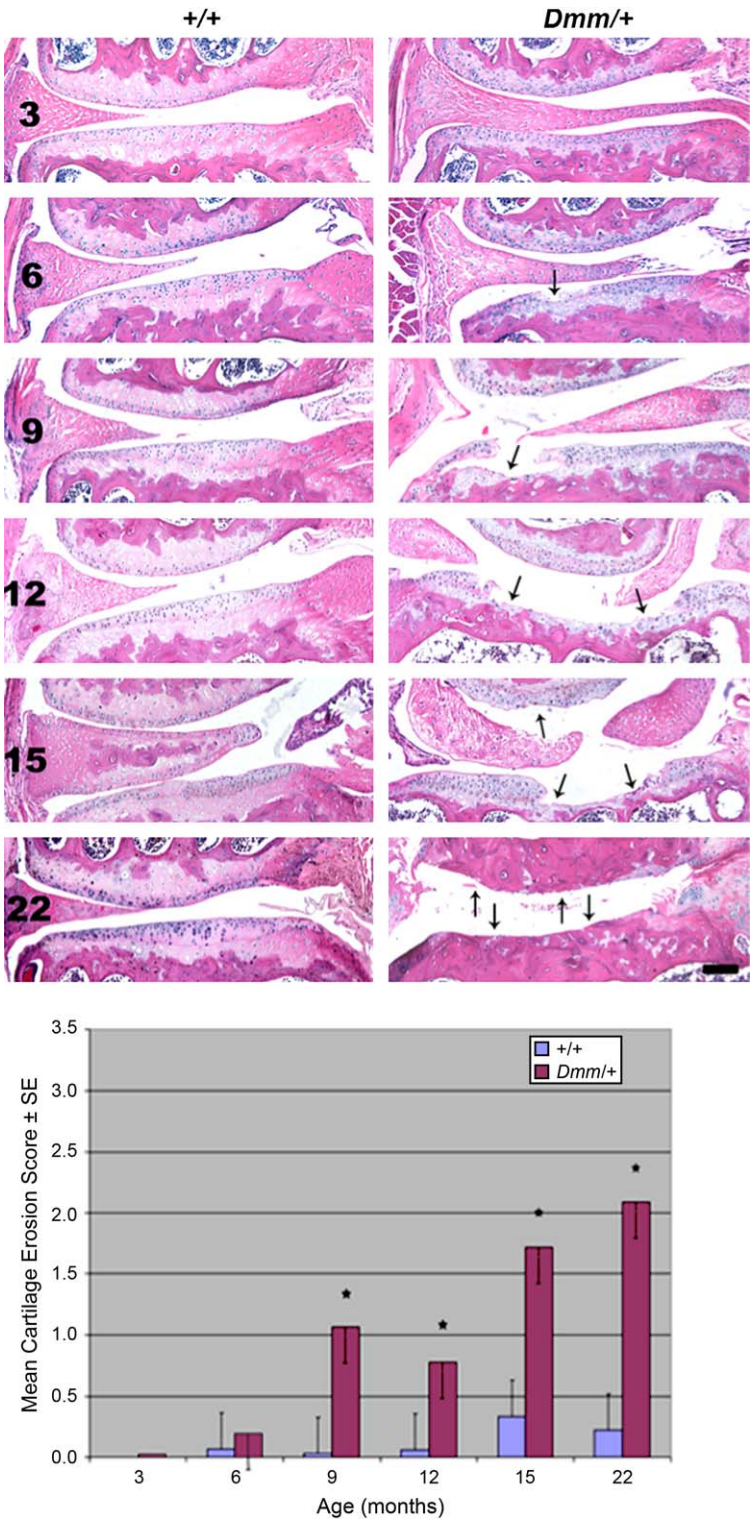

Fig. 2. *Dmm*/+ cartilage exhibited premature articular cartilage erosion. Images shown are low magnification (bar = 100 μm) light micrographs of medial knee joint cartilage. Numbers on the left side of the +/+ column indicate ages (months) of the mice. Knee joints from +/+ mice showed no irregularities in the cartilage until 15 months, when only superficial irregularities were seen. *Dmm*/+ joints showed erosion (arrows) of uncalcified cartilage as early as 6 months, and severity of erosion increased with age, eventually leading to complete loss of all cartilage. Quantification of cartilage erosion (lower panel) using the scoring system outlined in Table I revealed that average cartilage erosion in *Dmm*/+ articular cartilage is significantly greater than in +/+. $N = 4$ at each age and genotype, except $N = 5$ for 3-month +/+ and 3-month *Dmm*/+. $^{*}P < 0.05$.

subchondral bone by 15 months. Quantification of the degree of cartilage erosions using the scoring system shown in Table I confirmed that erosion of +/+ cartilage was minimal through 12 months and only slight increases were seen thereafter (Fig. 2). In contrast, erosion of *Dmm*/+ cartilage was evident in young mice and progressed steadily throughout adulthood, with significantly more erosion than in +/+ cartilage starting at 9 months of age.

CARTILAGE THINNING IN *DMM*/+ MICE

Under low magnification, the +/+ knee joints showed healthy cartilage with columnar arrays of chondrocytes and abundant ECM. *Dmm*/+ knee cartilage appeared thinner than +/+ cartilage and also displayed a lack of columnar organization of chondrocytes and a diminished amount of ECM between cells [Fig. 3(A)]. Quantification of total cartilage thickness revealed that *Dmm*/+ cartilage was significantly thinner than +/+ cartilage at all ages [Fig. 3(B)]. The

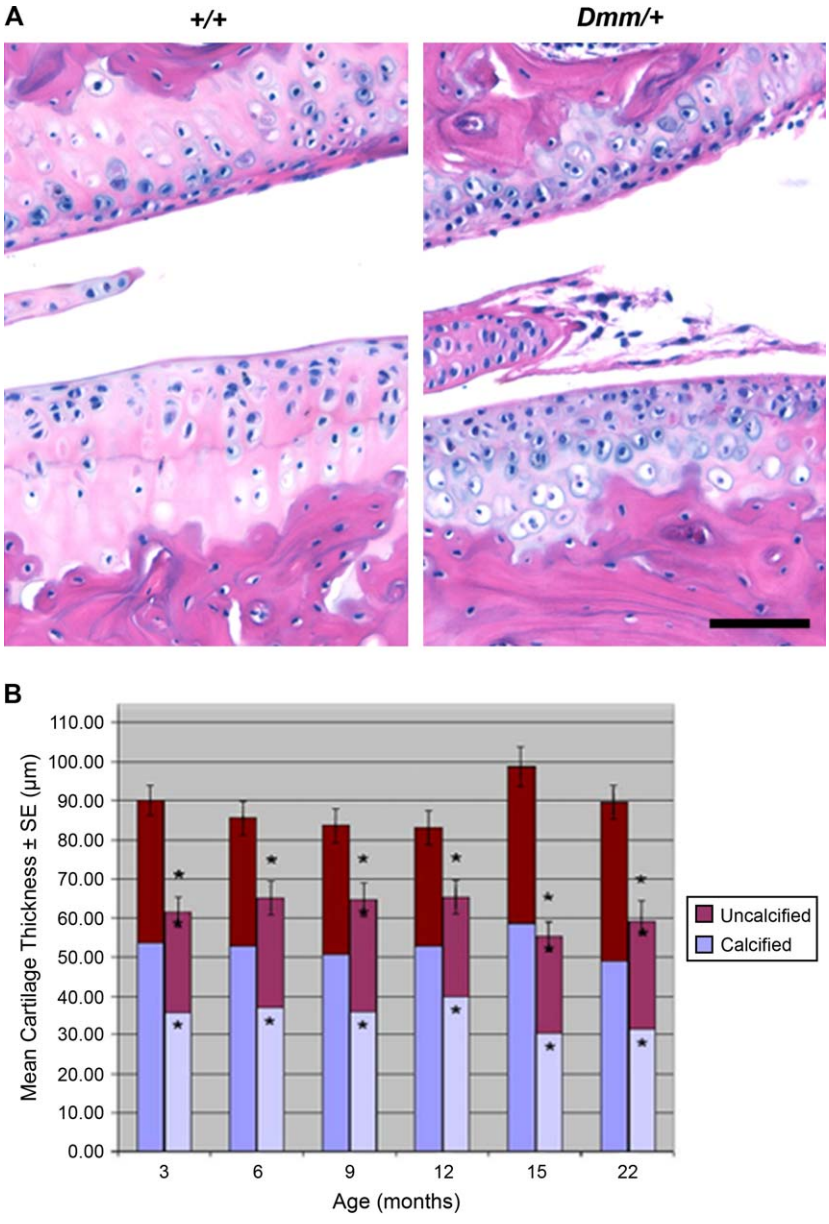

Fig. 3. Articular cartilage in *Dmm*/+ knee joints exhibited decreased thickness and disorganized arrangement of cells. (A) High magnification (bar = 50 μm) light micrographs of 6-month knee joints stained with hematoxylin and eosin revealed that +/+ articular cartilage had columnar arrays of chondrocytes while *Dmm*/+ cartilage was thinner than +/+ cartilage, lacked columnar organization of chondrocytes, and showed increased cell density. (B) Quantification of the average cartilage thickness revealed that *Dmm*/+ articular cartilage is significantly reduced relative to +/+ at every age examined. Left bar of each age group represents +/+, and right bar of each age group represents *Dmm*/+. Error bars and asterisks above the bar are for total cartilage thickness. Asterisks in the calcified or uncalcified portion of the bar are for the corresponding portion of the cartilage. $N = 4$ at each age and genotype, except $N = 5$ for 3-month +/+ and 3-month *Dmm*/+. $^*P < 0.05$.

calcified cartilage was also significantly thinner in *Dmm*/+ than in +/+ at all ages, as was uncalcified cartilage at all ages except 6 and 12 months.

INCREASED OA SCORING IN *DMM*/+ MICE

Safranin O is a cationic stain with a high affinity for negatively charged proteoglycan. In the modified Mankin scoring system for OA severity utilized here (Table I), reduced IMS by safranin O is indicative of proteoglycan deficiency. Furthermore, enhanced PMS suggests that chondrocytes have increased production and secretion of proteoglycan in response to proteoglycan degradation. Scoring of the spatial arrangement of cells is designed to detect disorganized chondrocyte proliferation, in early stages of OA, as well as cell death, in late stages of OA.

Fast green and safranin O-stained +/+ cartilage generally revealed evenly stained interterritorial matrix with normal levels of pericellular staining and columnar organization of chondrocytes [Fig. 4(A)]. In contrast, *Dmm*/+ cartilage frequently revealed regions of the interterritorial matrix with little or no proteoglycan staining, while also displaying enhanced staining of the pericellular matrix. The lack of organization and increased density of chondrocytes in *Dmm*/+ cartilage were also apparent in these sections. Modified Mankin scoring of these characteristics confirmed that *Dmm*/+ cartilage was in a more osteoarthritic state than +/+ at every age examined [Fig. 4(B)]. Furthermore, *Dmm*/+ cartilage had a significantly larger sub-score for each of the criteria (IMS, PMS, and spatial arrangement of cells) in virtually every age group when compared with +/+.

The IMS sub-scores from *Dmm*/+ cartilage revealed that proteoglycan deficiency was present at 3 months. Interestingly, however, this proteoglycan deficiency did not seem to increase with age [Fig. 4(B)]. The PMS sub-scores showed that *Dmm*/+ cartilage had areas of enhanced proteoglycan production as early as 3 months, which increased in size with age. A similar pattern of enhanced proteoglycan production was seen in +/+ cartilage, but not until later in life. The sub-scores for spatial arrangement of cells in *Dmm*/+ tissue revealed that cartilage was already hypercellular in 3-month animals, and this hypercellularity persisted until about 15 months when regions of the cartilage became hypocellular. In comparison, +/+ cartilage showed only slight hypercellularity in older animals.

INCREASED CELL DENSITY AND REDUCED MATRIX FRACTION IN *DMM* CARTILAGE

Histological sections of resin-embedded +/+ cartilage stained with toluidine blue/azure II showed moderate cell density near the surface of the cartilage and decreased cell density in deeper layers [Fig. 5(A)]. *Dmm*/+ appeared to have a greater cell density than +/+ near the surface of the cartilage and through the entire depth of the cartilage, and also appeared to have a reduced amount of ECM when

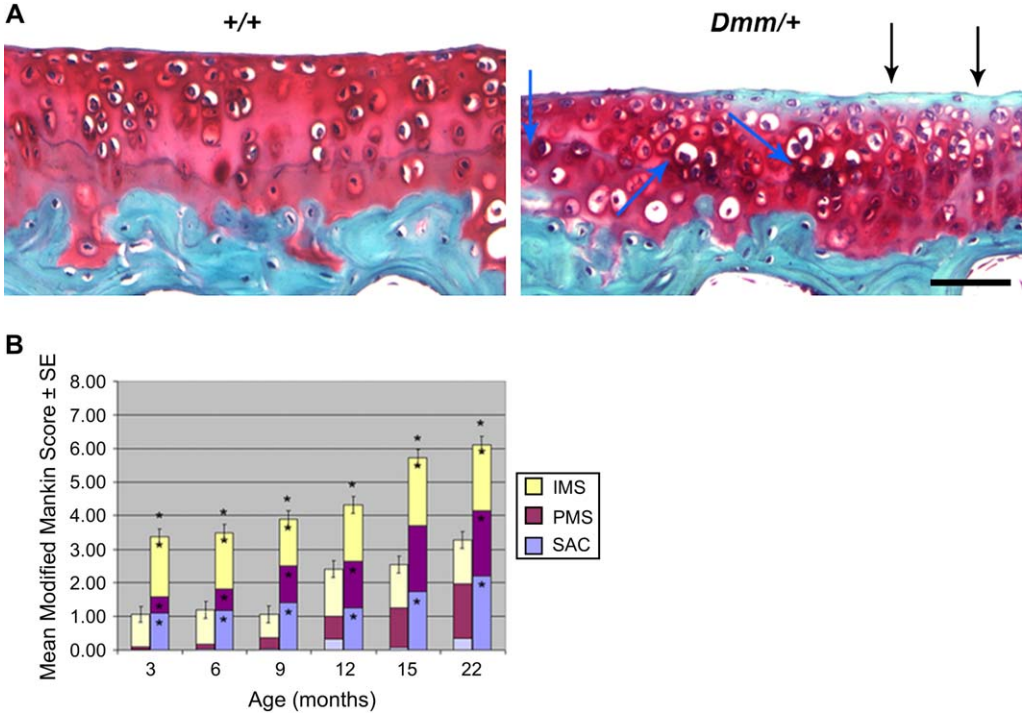

Fig. 4. Safranin O staining in *Dmm*/+ cartilage revealed regions of decreased proteoglycan staining in the interterritorial matrix and increased proteoglycan staining in the pericellular matrix. (A) Images shown are high magnification (bar = 50 μm) light micrographs of 9-month medial tibial cartilage, stained with fast green and safranin O. The +/+ cartilage displayed evenly stained interterritorial matrix with normal levels of pericellular staining and columnar organization of chondrocytes. In contrast, *Dmm*/+ cartilage contained regions of interterritorial matrix with little or no proteoglycan staining (black arrows), combined with enhanced staining of the pericellular matrix (blue arrows) and densely packed, disorganized chondrocytes. (B) Modified Mankin scoring revealed significantly more severe OA in *Dmm*/+ relative to +/+ cartilage. Left bar of each age group represents +/+, and right bar of each age group represents *Dmm*/+. Error bars and asterisks above the bar are for total score. Asterisks in the IMS, PMS, or SAC portion of the bar are for the corresponding sub-score. $N = 4$ at each age and genotype, except $N = 5$ for 3-month +/+ and 3-month *Dmm*/+. *Significantly greater than +/+ ($P < 0.05$).

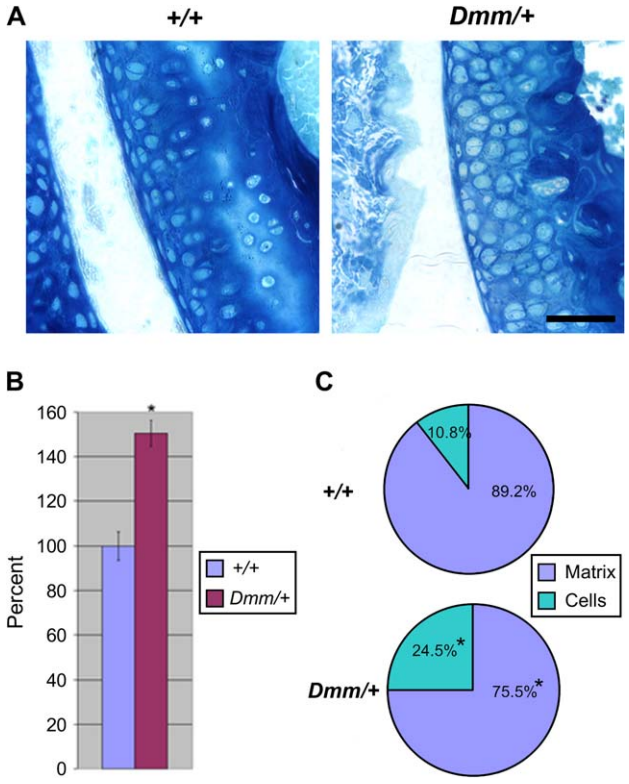

Fig. 5. *Dmm*/+ cartilage had increased cell density and decreased matrix fraction. (A) High magnification (bar = 50 μm) light micrographs of 3-month medial femoral cartilage stained with toluidine blue and azure II. Cartilage from +/+ mice showed moderate cell density near the surface of the cartilage and decreased cell density in deeper layers. *Dmm*/+, in contrast, showed increased cell density throughout the entire depth of the cartilage and a correspondingly reduced matrix fraction. (B) Cell counts showed 53% more cells per unit area in *Dmm*/+ than +/+ cartilage, even though *Dmm*/+ cells appeared to be larger (*$P < 0.01$). (C) Quantification of the relative area covered by cells vs ECM per unit area showed that *Dmm*/+ cartilage had a significantly decreased matrix fraction relative to +/+ cartilage. $N = 2$ for 3-month +/+ and *Dmm*/+, and for 6-month +/+. $N = 3$ for 6-month *Dmm*/+. (*$P < 0.01$).

compared to +/+. Quantification of these differences revealed that *Dmm*/+ mice have significantly more cells per unit area than +/+ [Fig. 5(B)]. The matrix fraction of +/+ cartilage was found to be 89.2%, whereas the matrix fraction of *Dmm*/+ cartilage was significantly less at 75.5% [Fig. 5(C)].

Discussion

This work has revealed that *Dmm*/+ mice display abnormalities in articular cartilage even at very young ages and before overt cartilage degeneration becomes apparent, presumably due to the role the *Dmm* mutation plays during cartilage development. These abnormalities include hypercellularity and decreased ECM fraction, which predispose the animals to severe premature articular cartilage degeneration.

The changes observed in *Dmm*/+ cartilage are consistent with a widely accepted three-stage model for the progression of OA. In the first stage, macromolecules in the ECM are degraded. Aggrecan, the major proteoglycan of cartilage, is cleaved by aggrecanases, and type II collagen, the major component of collagen fibrils, is cleaved by matrix metalloproteases[31–34]. The diminished matrix fraction observed in young *Dmm*/+ animals could result from such early-stage degradation of matrix molecules, but it more likely results from the decreased export of type II collagen, and perhaps other matrix macromolecules, from chondrocytes during the development of articular cartilage. Such decreased export of matrix molecules during development would result in the generation of significantly thinner articular cartilage in *Dmm*/+ relative to +/+ animals, with decreased ECM and increased crowding of the chondrocytes as was observed from the earliest time points measured. This thinness could in turn compromise the cartilage's ability to disperse compressive forces, thus increasing stress on the chondrocytes and evoking a chondrocytic inflammatory response, including the release of inflammatory cytokines known to promote the degradation of ECM macromolecules[1,35,36]. Accordingly, *Dmm*/+ mice as young as 3 months show significantly reduced proteoglycan staining in the interterritorial matrix relative to +/+ mice.

In the second stage of OA, chondrocytes attempt to replace the degraded ECM molecules by activating proliferative pathways as well as by increasing synthesis of new ECM macromolecules[1,37]. The increased proliferation produces cell clustering and hypercellularity, and the increased synthesis of ECM macromolecules produces concentrated proteoglycans in the immediate vicinity of the cell known as the pericellular matrix. In *Dmm*/+ mice, diffuse regions of cell clustering together with increased proteoglycan staining in the pericellular matrix were apparent and significantly different from +/+ as early as 3 months.

In the third stage of OA, irregularities initially appear as localized fibrillations in the superficial layer of articular cartilage. These abnormalities progress into deeper layers of the tissue, eventually leading to erosion of the cartilage. During the later stages of the disease, the chondrocytes' anabolic and proliferative responses are shut down. This, coupled with cell death, leads to hypocellularity of the tissue[1]. Erosion likely continues until cartilage is completely lost from articulating surfaces and the joint is left with only bone on bone interactions[1]. The majority of *Dmm*/+ mice progress into this third stage by 9 months, and the cartilage erosion becomes more and more severe over time. Several of the older *Dmm*/+ animals in this study displayed regions of erosion into and through the calcified cartilage, resulting in the exposure of subchondral bone. The +/+ mice, in contrast, rarely displayed any lesions worse than a roughening of the articular surface, even at 22 months.

It is interesting to note the severity of this OA phenotype in *Dmm*/+ animals, in spite of the fact that they also exhibit decreased body weight. (Our unpublished observations show that *Dmm*/+ mice weigh approximately 17% less than +/+ mice, on average.) This is in contrast to the case in humans, where increased body mass is thought to contribute to the development of OA. The more favorable weight-bearing conditions in *Dmm*/+ mice relative to +/+ mice are clearly not sufficient to counteract the effects of the *Dmm* mutation and the resulting cartilage defect, a situation that has parallels with some human OA sufferers.

Other parallels between *Dmm*/+, human OA, and other mouse models of OA are apparent. For example, in both *Dmm*/+ and STR/ort mice, the medial side of the knee joint exhibits more severe cartilage erosion than the lateral side[38]. This is presumably due to a joint structure that places more of the stress of walking on the medial portion of the joint. In humans, joint structure that results in the

uneven distribution of joint pressure also results in a predisposition to OA at the site of increased pressure[1].

In summary, human and *Dmm* OA tend to follow the three-stage progression outlined above, whether the OA is triggered by different genetic mutations, structural abnormalities, increased body mass, or other factors. The genetic basis for most human OA cases is unknown, but this similarity in the disease progression suggests that OA may follow a common pathway of molecular pathogenesis regardless of its initial trigger. This in turn suggests that much can be learned about human OA from the *Dmm* model, even though the majority of human OA cases are not caused by *COL2A1* mutations. Continuous study of *Dmm* mice in relation to other models and to human cases will reveal whether this common pathogenetic pathway hypothesis is correct. In the meantime, however, we conclude that the work presented here establishes *Dmm* mice as an appropriate model for studying OA disease progression and for testing potential treatments.

Acknowledgments

The authors are indebted to Dr James Porter of the Brigham Young University, Department of Physiology and Developmental Biology for assisting with the statistical analysis. The authors also thank John McCallister, Matthew Merrill, Shaela Willie, Scott Peterson, Dustin Griner, Jimmy MacDonald, and Lisa Higginbotham for procedural help.

References

1. Buckwalter JA, Mankin HJ. Articular cartilage: tissue design and chondrocyte–matrix interactions. Instr Course Lect 1998;47:477–86.
2. Bendele AM. Animal models of osteoarthritis in an era of molecular biology. J Musculoskelet Neuronal Interact 2002;2:501–3.
3. Marijnissen AC, van Roermund PM, TeKoppele JM, Bijlsma JW, Lafeber FP. The canine 'groove' model, compared with the ACLT model of osteoarthritis. Osteoarthritis Cartilage 2002;10:145–55.
4. Marijnissen AC, van Roermund PM, Verzijl N, Tekoppele JM, Bijlsma JW, Lafeber FP. Steady progression of osteoarthritic features in the canine groove model. Osteoarthritis Cartilage 2002;10:282–9.
5. Bendele AM. Animal models of osteoarthritis. J Musculoskelet Neuronal Interact 2001;1:363–76.
6. Wagner M, Werner A, Grunder W. Visualization of collagenase-induced cartilage degradation using NMR microscopy. Invest Radiol 1999;34:607–14.
7. Walton M. Studies of degenerative joint disease in the mouse knee joint; scanning electron microscopy. J Pathol 1977;123:211–7.
8. Walton M. Degenerative joint disease in the mouse knee; radiological and morphological observations. J Pathol 1977;123:97–107.
9. Walton M. Degenerative joint disease in the mouse knee; histological observations. J Pathol 1977;123: 109–22.
10. Metsaranta M, Garofalo S, Decker G, Rintala M, de Crombrugghe B, Vuorio E. Chondrodysplasia in transgenic mice harboring a 15-amino acid deletion in the triple helical domain of pro alpha 1(II) collagen chain. J Cell Biol 1992;118:203–12.
11. Saamanen AK, Salminen HJ, Dean PB, De Crombrugghe B, Vuorio EI, Metsaranta MP. Osteoarthritis-like lesions in transgenic mice harboring a small deletion mutation in type II collagen gene. Osteoarthritis Cartilage 2000;8:248–57.
12. Li Y, Lacerda DA, Warman ML, Beier DR, Yoshioka H, Ninomiya Y, *et al*. A fibrillar collagen gene, Col11a1, is essential for skeletal morphogenesis. Cell 1995;80: 423–30.
13. Rodriguez RR, Seegmiller RE, Stark MR, Bridgewater LC. A type XI collagen mutation leads to increased degradation of type II collagen in articular cartilage. Osteoarthritis Cartilage 2004;12:314–20.
14. Xu L, Flahiff CM, Waldman BA, Wu D, Olsen BR, Setton LA, *et al*. Osteoarthritis-like changes and decreased mechanical function of articular cartilage in the joints of mice with the chondrodysplasia gene (cho). Arthritis Rheum 2003;48:2509–18.
15. Brown KS, Cranley RE, Greene R, Kleinman HK, Pennypacker JP. Disproportionate micromelia (Dmm): an incomplete dominant mouse dwarfism with abnormal cartilage matrix. J Embryol Exp Morphol 1981;62:165–82.
16. Foster MJ, Caldwell AP, Staheli J, Smith DH, Gardner JS, Seegmiller RE. Pulmonary hypoplasia associated with reduced thoracic space in mice with disproportionate micromelia (DMM). Anat Rec 1994; 238:454–62.
17. Ricks JE, Ryder VM, Bridgewater LC, Schaalje B, Seegmiller RE. Altered mandibular development precedes the time of palate closure in mice homozygous for disproportionate micromelia: an oral clefting model supporting the Pierre-Robin sequence. Teratology 2002;65:116–20.
18. Pace JM, Li Y, Seegmiller RE, Teuscher C, Taylor BA, Olsen BR. Disproportionate micromelia (Dmm) in mice caused by a mutation in the C-propeptide coding region of Col2a1. Dev Dyn 1997;208:25–33.
19. Lamande SR, Bateman JF. Procollagen folding and assembly: the role of endoplasmic reticulum enzymes and molecular chaperones. Semin Cell Dev Biol 1999;10:455–64.
20. Tasab M, Batten MR, Bulleid NJ. Hsp47: a molecular chaperone that interacts with and stabilizes correctly-folded procollagen. EMBO J 2000;19:2204–11.
21. Blaschke UK, Eikenberry EF, Hulmes DJ, Galla HJ, Bruckner P. Collagen XI nucleates self-assembly and limits lateral growth of cartilage fibrils. J Biol Chem 2000;275:10370–8.
22. Pace JM, Kuslich CD, Willing MC, Byers PH. Disruption of one intra-chain disulphide bond in the carboxyl-terminal propeptide of the proalpha1(I) chain of type I procollagen permits slow assembly and secretion of overmodified, but stable procollagen trimers and results in mild osteogenesis imperfecta. J Med Genet 2001;38:443–9.
23. Fernandes RJ, Seegmiller RE, Nelson WR, Eyre DR. Protein consequences of the Col2a1 C-propeptide mutation in the chondrodysplastic Dmm mouse. Matrix Biol 2003;22:449–53.
24. Kuivaniemi H, Tromp G, Prockop DJ. Mutations in fibrillar collagens (types I, II, III, and XI), fibril-associated collagen (type IX), and network-forming collagen (type X) cause a spectrum of diseases of bone, cartilage, and blood vessels. Hum Mutat 1997;9:300–15.
25. Ahmad NN, Dimascio J, Knowlton RG, Tasman WS. Stickler syndrome. A mutation in the nonhelical 3′

end of type II procollagen gene. Arch Ophthalmol 1995;113:1454–7.
26. Richards AJ, Morgan J, Bearcroft PW, Pickering E, Owen MJ, Holmans P, *et al*. Vitreoretinopathy with phalangeal epiphyseal dysplasia, a type II collagenopathy resulting from a novel mutation in the C-propeptide region of the molecule. J Med Genet 2002;39:661–5.
27. Winterpacht A, Superti-Furga A, Schwarze U, Stoss H, Steinmann B, Spranger J, *et al*. The deletion of six amino acids at the C-terminus of the alpha 1 (II) chain causes overmodification of type II and type XI collagen: further evidence for the association between small deletions in COL2A1 and Kniest dysplasia. J Med Genet 1996;33:649–54.
28. Mortier GR, Weis M, Nuytinck L, King LM, Wilkin DJ, De Paepe A, *et al*. Report of five novel and one recurrent COL2A1 mutations with analysis of genotype–phenotype correlation in patients with a lethal type II collagen disorder. J Med Genet 2000;37:263–71.
29. Unger SL, Briggs MD, Holden P, Zabel B, Ala-Kokko L, Paassilta P, *et al*. Multiple epiphyseal dysplasia: radiographic abnormalities correlated with genotype. Pediatr Radiol 2001;31:10–8.
30. Lippiello L, Hall D, Mankin HJ. Collagen synthesis in normal and osteoarthritic human cartilage. J Clin Invest 1977;59:593–600.
31. Arner EC. Aggrecanase-mediated cartilage degradation. Curr Opin Pharmacol 2002;2:322–9.
32. Ehrlich MG, Armstrong AL, Treadwell BV, Mankin HJ. The role of proteases in the pathogenesis of osteoarthritis. J Rheumatol 1987;14(Spec No):30–2.
33. Flannelly J, Chambers MG, Dudhia J, Hembry RM, Murphy G, Mason RM, *et al*. Metalloproteinase and tissue inhibitor of metalloproteinase expression in the murine STR/ort model of osteoarthritis. Osteoarthritis Cartilage 2002;10:722–33.
34. Kostoulas G, Lang A, Nagase H, Baici A. Stimulation of angiogenesis through cathepsin B inactivation of the tissue inhibitors of matrix metalloproteinases [published erratum appears in FEBS Lett 2000 Jan 28; 466(2–3):394]. FEBS Lett 1999;455:286–90.
35. Walker JA, Molloy SS, Thomas G, Sakaguchi T, Yoshida T, Chambers TM, *et al*. Sequence specificity of furin, a proprotein-processing endoprotease, for the hemagglutinin of a virulent avian influenza virus. J Virol 1994;68:1213–8.
36. Goldring SR, Goldring MB. The role of cytokines in cartilage matrix degeneration in osteoarthritis. Clin Orthop Relat Res 2004;S27–36.
37. Cs-Szabo G, Roughley PJ, Plaas AH, Glant TT. Large and small proteoglycans of osteoarthritic and rheumatoid articular cartilage. Arthritis Rheum 1995;38:660–8.
38. Mason RM, Chambers MG, Flannelly J, Gaffen JD, Dudhia J, Bayliss MT. The STR/ort mouse and its use as a model of osteoarthritis. Osteoarthritis Cartilage 2001;9:85–91.